

Synthesis and Characterization of Mononuclear Bis(para-substituted phenolato)oxomolybdenum(V) Complexes: Dependence of the Molecular Properties upon Remote Substituent Effects

Chung-Sheng J. Chang,^{1a,b} Tonia J. Pecci,^{1c} Michael D. Carducci,^{1a} and John H. Enemark^{*,1a}

Department of Chemistry, University of Arizona, Tucson, Arizona 85721

Received December 3, 1992[®]

Bis(para-substituted phenolato)oxomolybdenum(V) complexes with the general formula $\text{LMoO}(\text{OC}_6\text{H}_4\text{X})_2$, where L = hydrotris(3,5-dimethyl-1-pyrazolyl)borate and X = Me, Et, OMe, OEt, OH, F, Cl, Br, I, and CN, have been prepared and characterized by elemental analyses, mass spectrometry, and IR, EPR, and UV-vis-near-IR spectroscopy. The energies of both the ligand-field and the lowest-energy charge-transfer bands depend upon the σ_p values of the para substituents (X) on the phenolato ligands. Compared with $\text{LMoO}(\text{OC}_6\text{H}_5)_2$, the absorption energies of compounds with electron-donating substituents exhibit bathochromic shifts, whereas compounds with electron-withdrawing substituents show hypsochromic shifts. The anisotropic spin Hamiltonian g_i values are similar for all members of the series. The X-ray crystal structure of $\text{LMoO}(\text{OC}_6\text{H}_4\text{Me})_2$ has been determined and is similar to previously determined structures in the general class of $\text{LMoO}(\text{EC}_6\text{H}_4\text{X})_2$ (E = O, S) compounds.

Introduction

The presence of an oxo-molybdenum center² in a variety of enzymes such as sulfite oxidase (SO), nitrate reductase (NR), and xanthine oxidase (XO) that catalyze the formal transfer of an oxygen atom (eq 1) has stimulated research on molybdenum



complexes that mimic the reported spectroscopic properties or chemical reactions of molybdoenzymes.^{3–7} However, to date, the effects of changes in ligand substituents *outside* of the molybdenum coordination sphere upon the properties of the molybdenum center have received little attention.⁸

Recent physical and chemical measurements of a series of mononuclear monooxomolybdenum(V) complexes containing dithiolato, diolato, alkoxy, or alkanethiolato ligands have shown^{9–11} that both geometric and inductive factors can influence the extent of ligand-to-molybdenum $p_\pi-d_\pi$ interactions and hence the energy of the molybdenum-based orbitals. Geometric effects gave greater changes in π -interaction than inductive effects.^{9,10}

Here we describe the syntheses and characterization of a series of mononuclear bis(para-substituted phenolato)oxomolybdenum(V) complexes, $\text{LMoO}(\text{OC}_6\text{H}_4\text{X})_2$, (Figure 1). The remote para substituents (X) on the $(\text{OC}_6\text{H}_4\text{X})_2$ ligands of these compounds are expected to have little or no steric influence on the coordination geometry about the Mo center. Consequently, the electronic effects of the para substituent on the ligand-to-

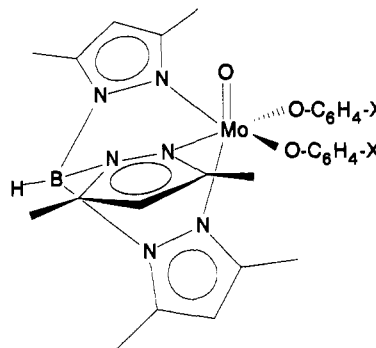


Figure 1. Schematic structure of the $\text{LMoO}(\text{OC}_6\text{H}_4\text{X})_2$ compounds.

molybdenum $p_\pi-d_\pi$ interaction can be systematically investigated by optical and EPR spectroscopy.

Experimental Section

Materials. Solvents were thoroughly degassed and purified by distillation under an inert atmosphere of dry nitrogen before use; 1,2-dichloroethane and dichloromethane from calcium hydride; benzene, toluene, and tetrahydrofuran from potassium/benzophenone; triethylamine from potassium. Potassium hydrotris(3,5-dimethyl-1-pyrazolyl)borate (KL) and dichloro(hydrotris(3,5-dimethyl-1-pyrazolyl)borato)oxomolybdenum(V) (LMoOCl_2) were prepared according to literature methods.^{12,13} The phenols were purchased from Aldrich Chemical Co. and sublimed before use. Reactions were carried out under an inert atmosphere of pure dry nitrogen using standard Schlenk technique. Subsequent workup of the product was carried out in air. Elemental analyses were performed by Atlantic Microlab Inc. or Huffman Laboratories, Inc.

Compound Syntheses. To a stirred LMoOCl_2 solution (0.50 g, 1.0 mmol, in 60 mL of benzene or toluene) containing 0.5 g of dry MgSO_4 in a 100-mL airless flask at 40 °C was slowly added 15 mL of a benzene or toluene solution containing 3.0 mmol of triethylamine and 2.3 mmol of the appropriate phenol. The reaction mixture was heated gradually to 70–75 °C and maintained at that temperature until completion of the reaction (typically 4–9 h). The purity of isolated compounds as well as the progress of the reactions was monitored by thin-layer chromatography and EPR. Upon completion, the reaction mixture was cooled to room

- * Abstract published in *Advance ACS Abstracts*, August 15, 1993.
- (1) (a) University of Arizona. (b) Present address: Catalyst Research Center, China Technical Consultants, Inc., Box 88, Tofuen, Taiwan, Republic of China. (c) Summer NSF-REU participant from Marlboro College, Marlboro, VT 05344.
 - (2) Cramer, S. P.; Stiefel, E. I. In *Molybdenum Enzymes*; Spiro, T. G., Ed.; Wiley: New York, 1985; Chapter 8, pp 411–441.
 - (3) Spiro, T. G., Ed. *Molybdenum Enzymes*; Wiley: New York, 1985.
 - (4) Spence, J. T. *Coord. Chem. Rev.* **1983**, *48*, 59.
 - (5) Burgmayer, S. J. N.; Stiefel, E. I. *J. Chem. Educ.* **1985**, *62*, 943.
 - (6) Bray, R. C. *Q. Rev. Biophys.* **1988**, *21*, 299.
 - (7) Holm, R. H. *Coord. Chem. Rev.* **1990**, *110*, 183.
 - (8) Topich, J. *Inorg. Chem.* **1981**, *20*, 3704–3707.
 - (9) Chang, C. S. J.; Collison, D.; Mabbs, F. E.; Enemark, J. H. *Inorg. Chem.* **1990**, *29*, 2261–2267.
 - (10) Chang, C. S. J.; Lichtenberger, D. L.; Enemark, J. H. *Polyhedron* **1990**, *9*, 1965–1973.
 - (11) Chang, C. S. J.; Enemark, J. H. *Inorg. Chem.* **1991**, *30*, 683–688.

- (12) Trofimenko, S. J. *J. Am. Chem. Soc.* **1967**, *89*, 6288–6294.
- (13) Cleland, W. E., Jr.; Barnhart, K. M.; Yamanouchi, K.; Collison, D.; Mabbs, F. E.; Ortega, R. B.; Enemark, J. H. *Inorg. Chem.* **1987**, *26*, 1017–1025.

temperature, filtered, evaporated to dryness in vacuo, redissolved in a minimum amount of dichloromethane, and chromatographed on a silica gel column.

LMO(OC₆H₄Me)₂ (1). The color of the reaction solution changed from green to dark red. The crude reaction mixture was chromatographed on silica gel with benzene. The desired compound was eluted as a dark ruby-red band, evaporated to dryness, and recrystallized from benzene. Yield was 95%. Anal. Calcd for C₂₉H₃₆BN₆O₃Mo (MW 623.39): C, 55.87; H, 5.82; N, 13.48. Found: C, 56.31; H, 6.00; N, 12.98. MS: 623 [MP]⁺, 516 [MP - (OC₆H₄Me)]⁺, 411 [MP - 2(OC₆H₄Me)]⁺. IR: $\nu_{(\text{MoO})}$ 937 cm⁻¹.

LMO(OC₆H₄Et)₂ (2). The preparation of this compound was identical to that described for 1. The yield was 87%. Anal. Calcd for C₃₁H₄₀BN₆O₃Mo (MW 651.44): C, 57.16; H, 6.19; N, 12.90. Found: C, 57.38; H, 6.33; N, 12.79. MS: 652 [MP]⁺, 567 [MP - (OC₆H₄Et)]⁺, 411 [MP - 2(OC₆H₄Et)]⁺. IR: $\nu_{(\text{MoO})}$ 933 cm⁻¹.

LMO(OC₆H₄OMe)₂ (3). To prevent any photochemical reaction from occurring, all manipulations were performed under light-free conditions. The crude reaction mixture was chromatographed on silica gel with 1:1 (v/v) dichloromethane-benzene. The desired compound was eluted as a dark brown band and was evaporated to dryness; the yield was 86%. Anal. Calcd for C₂₉H₃₆BN₆O₃Mo (MW 655.39): C, 53.15; H, 5.54; N, 12.82. Found: C, 55.08; H, 6.22; N, 11.99. MS: 655 [MP]⁺, 534 [MP - (OC₆H₄OMe)]⁺, 411 [MP - 2(OC₆H₄OMe)]⁺. IR: $\nu_{(\text{MoO})}$ 933 cm⁻¹.

LMO(OC₆H₄OEt)₂ (4). The preparation of this compound was identical to that for 3. The yield was 87%. Anal. Calcd for C₃₁H₄₀BN₆O₄Mo (MW 683.44): C, 54.48; H, 5.90; N, 12.30. Found: C, 55.13; H, 5.97; N, 12.18. MS: 685 [MP]⁺, 546 [MP - (OC₆H₄OEt)]⁺, 411 [MP - 2(OC₆H₄OEt)]⁺. IR: $\nu_{(\text{MoO})}$ 936 cm⁻¹.

LMO(OC₆H₄OH)₂ (5). All manipulations for this compound were performed under light-free conditions. The desired compound was chromatographed on silica gel and eluted with 1:1 (v/v) tetrahydrofuran-toluene as a brownish fraction. The yield was 77%. Anal. Calcd for C₂₇H₃₂BN₆O₅Mo (MW 627.34): C, 51.69; H, 5.14; N, 13.40. Found: C, 54.18; H, 5.60; N, 12.36. MS: 414 [MP - 2(OC₆H₄OH)]⁺. IR: $\nu_{(\text{MoO})}$ 934 cm⁻¹.

LMO(OC₆H₄F)₂ (6). The crude reaction mixture was chromatographed with benzene. The desired compound was eluted as a dark red band, which was evaporated to dryness. The yield was 84%. Anal. Calcd for C₂₇H₃₀BF₂N₆O₃Mo (MW 631.32): C, 51.37; H, 4.79; N, 13.31; F, 6.02. Found: C, 51.18; H, 4.85; N, 13.19; F, 4.68. MS: 633 [MP]⁺, 520 [MP - (OC₆H₄F)]⁺, 411 [MP - 2(OC₆H₄F)]⁺. IR: $\nu_{(\text{MoO})}$ 938 cm⁻¹.

LMO(OC₆H₄Cl)₂ (7). The purification of this compound was identical to that for 6. The yield was 85%. Anal. Calcd for C₂₇H₃₀BCl₂N₆O₃Mo (MW 644.23): C, 48.82; H, 4.55; N, 12.65; Cl, 10.67. Found: C, 48.81; H, 4.60; N, 12.56; Cl, 10.62. MS: 665 [MP]⁺, 538 [MP - (OC₆H₄Cl)]⁺, 411 [MP - 2(OC₆H₄Cl)]⁺. IR: $\nu_{(\text{MoO})}$ 937 cm⁻¹.

LMO(OC₆H₄Br)₂ (8). The purification of this compound was identical to that for 6. The yield was 85%. Anal. Calcd for C₂₇H₃₀BBR₂N₆O₃Mo (MW 753.13): C, 43.06; H, 4.01; N, 11.16; Br, 21.22. Found: C, 43.57; H, 4.19; N, 10.84; Br, 20.89. MS: 753 [MP]⁺, 582 [MP - (OC₆H₄Br)]⁺, 410 [MP - 2(OC₆H₄Br)]⁺. IR: $\nu_{(\text{MoO})}$ 939 cm⁻¹.

LMO(OC₆H₄I)₂ (9). The purification of this compound was identical to that for 6. The yield was 50%. Anal. Calcd for C₂₇H₃₀BI₂N₆O₃Mo (MW 847.13): C, 38.28; H, 3.57; N, 9.92; I, 29.96. Found: C, 39.75; H, 4.22; N, 9.98; I, 27.92. MS: 846 [MP]⁺, 629 [MP - (OC₆H₄I)]⁺, 409 [MP - 2(OC₆H₄I)]⁺. IR: $\nu_{(\text{MoO})}$ 940 cm⁻¹.

LMO(OC₆H₄CN)₂ (10). The crude reaction mixture was chromatographed with 1:1 (v/v) dichloromethane-benzene. The orange eluent was collected and evaporated to dryness. The yield was 85%. Anal. Calcd for C₂₉H₃₀BN₆O₃Mo (MW 645.36): C, 53.97; H, 4.69; N, 17.36. Found: C, 53.76; H, 4.65; N, 17.22. MS: 647 [MP]⁺, 526 [MP - (OC₆H₄CN)]⁺, 409 [MP - 2(OC₆H₄CN)]⁺. IR: $\nu_{(\text{MoO})}$ 945 cm⁻¹.

Physical Measurements. Mass spectra were obtained with a Finnigan 3300 quadrupole gas chromatographic/mass spectrometer (GC/MS) with a INCOS data system or a Hewlett Packard 5988A quadrupole GC/MS with a RTE-6 data system. Most compounds were ionized by electron impact at 70 eV; compound 9 was ionized by chemical ionization using isobutane. Infrared spectra of the powdered samples (KBr pellets) in the 4000–250-cm⁻¹ region were taken using a Perkin-Elmer PE 983 spectrometer. Electron paramagnetic resonance spectra of the fluid solutions (at room temperature) or frozen glasses in toluene (at liquid

Table I. Selected Bond Distances and Bond Angles for (1)^a

Distances (Å)			
Mo=O2	1.677(3)	Mo-N21	2.169(4)
Mo-O1	1.954(3)	Mo-N31	2.163(3)
Mo-O3	1.928(3)	O1-C41	1.360(5)
Mo-N11	2.334(4)	O3-C51	1.340(6)
Angles (deg)			
O1-Mo-O3	90.9(1)	O2-Mo-N21	92.6(2)
O2-Mo-O1	100.2(1)	O2-Mo-N31	91.4(2)
O2-Mo-O3	103.5(2)	Mo-O1-C41	130.5(3)
O2-Mo-N11	168.6(1)	Mo-O3-C51	145.9(3)

^a Estimated standard deviations in the least significant figure are given in parentheses.

nitrogen temperature) were recorded at X-band frequencies using a Varian E-3 spectrometer. All of the EPR spectra were calibrated with DPPH (α, α' -diphenyl- β -picrylhydrazyl). Electronic absorption spectra were obtained on an OLIS 4300S modified Cary-14 UV/vis/near-IR spectrophotometer or on an IBM 9420 spectrophotometer.

Results and Discussion

Properties of 1–10. All of the compounds are stable to air and moisture. The compounds do not react with carbon disulfide, and no insertion products could be detected. This behavior is different from that of most transition-metal complexes containing an M-OR moiety.¹⁴ The bulky hydrotris(3,5-dimethyl-1-pyrazolyl)borate ligand may be responsible for the low reactivity.

Characterization. The low-resolution mass spectral data (Experimental Section) support the mononuclear formulation for these complexes. The reported mass number for each compound refers to the peak of maximum intensity within the multiplet around the parent ion peak. Compounds 1–4 and 6–10 exhibit several common features: (a) the molecular ion peaks [MP]⁺, (b) the ion peaks [MP - (OC₆H₄X)]⁺, (c) the ion peaks [MP - 2(OC₆H₄X)]⁺, and (d) the ion peaks [OC₆H₄X]⁺. In addition, complexes 1–10 have a peak at $m/z = 96$, which can be assigned to a displaced 3,5-dimethylpyrazole ring.

Infrared Spectra. All of the compounds exhibit the characteristic bands of the hydrotris(3,5-dimethyl-1-pyrazolyl)borate ligand ($\nu_{\text{B-H}} = 2536\text{--}2547\text{ cm}^{-1}$) and a strong Mo=O stretch ($\nu_{\text{Mo=O}} = 933\text{--}945\text{ cm}^{-1}$) at a lower frequency than that of LMOCl₂ ($\nu_{\text{Mo=O}} = 961\text{ cm}^{-1}$). The reduced bond order between the molybdenum atom and the terminal oxygen atom¹⁵ for these phenolate derivatives suggests that the phenolate ligands are also good π -donors to the vacant d_x orbitals of the metal. Compound 10, containing 4-cyanophenolate, exhibits the highest stretching frequency for the Mo=O bond (945 cm⁻¹). Similar results are also observed in many other systems; for example, in the series [MoO(SR)₄]⁻ (R = C₆H₅, C₁₀H₇, 4-CH₃C₆H₄, 3-ClC₆H₄, 2,6-Cl₂C₆H₃, C₆F₅), $\nu_{\text{Mo=O}}$ shifts to higher frequencies as the electron-withdrawing nature of the substituents increases.¹⁶

Crystallographic Analysis of LMO(OC₆H₄Me)₂ (1). Selected structural parameters from the X-ray crystal structure¹⁷ of compound 1 are listed in Table I. As depicted in Figure 2, the tridentate hydrotris(3,5-dimethyl-1-pyrazolyl)borate ligand occupies one face of the distorted octahedron about molybdenum while the terminal oxo group and the two 4-methylphenolato ligands occupy the other three mutually cis coordination sites.

(14) (a) Bradley, D. C.; Gaur, P. D.; Mehrota, R. C. *Metal Alkoxides*; Academic Press: London, 1978. (b) Bradley, D. C.; Chisholm, M. H. *Acc. Chem. Res.* 1976, 9, 273–280.

(15) Nugent, W. A.; Mayer, J. M. *Metal-Ligand Multiple Bonds*; Wiley: New York, 1988.

(16) Garner, C. D.; Hill, L.; Howlader, N. C.; Hyde, M. R.; Mabbs, F. E.; Routledge, V. I. *J. Less-Common Met.* 1977, 54, 27–34.

(17) Crystal Data for compound 1 (C₂₉H₃₆BN₆O₃Mo): dark brown-red rhomboids, triclinic, P1 (No. 2), $a = 10.703(3)\text{ \AA}$, $b = 12.133(3)\text{ \AA}$, $c = 13.678(4)\text{ \AA}$, $\alpha = 87.94(2)^\circ$, $\beta = 69.72(2)^\circ$, $\gamma = 65.68(2)^\circ$, $V = 1506.3\text{ \AA}^3$, $Z = 2$, $f_w = 623.40\text{ g mol}^{-1}$, $D(\text{calc}) = 1.37\text{ g cm}^{-3}$, $\mu(\text{Mo K}\alpha) = 4.6\text{ cm}^{-1}$, $T = 23 \pm 1^\circ\text{C}$; 5779 total reflections (5355 unique) reflections with $2\theta_{\text{max}} = 50^\circ$ of which 4300 with $F_o^2 > 3\sigma(F_o^2)$ were included in the refinement. Final $R = 0.039$ and $R_w = 0.050$.

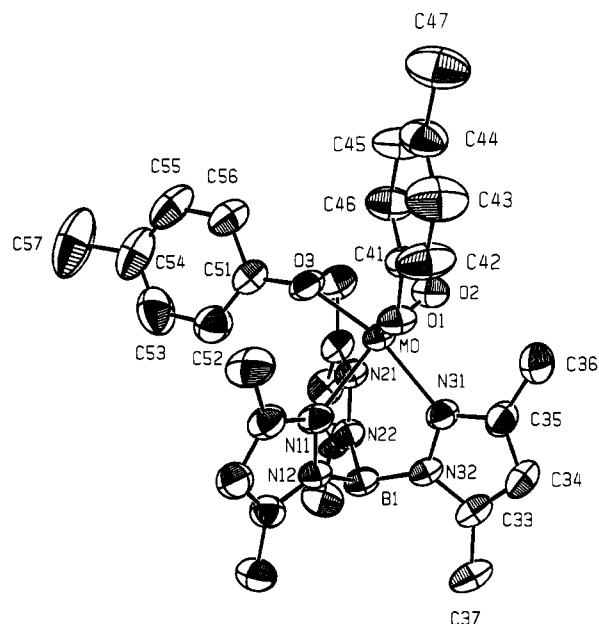


Figure 2. ORTEP drawing of compound **1** with 50% probability ellipsoids. The numbering of the atoms in the pyrazole rings containing N11 and N21 parallels that shown for the ring containing N31. Hydrogen atoms have been omitted.

The observed Mo=O distance of **1** is similar to that of $\text{LMoO}(\text{OC}_6\text{H}_4\text{X})_2$ ($\text{X} = \text{H}$ or Cl) and falls in the normal range ($1.677 \pm 0.048 \text{ \AA}$) reported for monooxomolybdenum(V) complexes.¹⁸ The bond lengths Mo–N21 and Mo–N31 are in the normal region of a single bond. However, the Mo–N11 bond is about 0.15 Å longer than that of Mo–N21 and Mo–N31, consistent with the strong trans-effect of a terminal oxo ligand.¹³ The structural parameters of the $[\text{LMoO}]^{+2}$ core are similar to those found for other oxomolybdenum(V) complexes.^{13,19–21}

The effective coordination symmetry of **1** is C_1 due to the different orientations of the two 4-methylphenolato groups. The phenyl ring of **1** containing O1 extends from the pocket that is formed by two 3-methyl groups of L. A similar orientation occurs for the single phenolate in the monophenolato compound $\text{LMoOCl}(\text{OC}_6\text{H}_4\text{CN})$.²² The other phenyl ring of **1** lies in the crease between two pyrazole rings of L (Figure 2). This overall stereochemistry has been found for other $\text{LMoO}(\text{OC}_6\text{H}_4\text{X})_2$ ($\text{X} = \text{H}$ or Cl) compounds^{19,20} and for $\text{LMoO}(\text{SC}_6\text{H}_5)_2$.¹³ For the three bis(para-substituted phenolato)oxomolybdenum(V) complexes ($p\text{-X} = \text{Me}$, H , or Cl) that have been structurally characterized, the Mo–O1 bond length of the phenolato ligand that extends away from the pocket formed by L is slightly longer (3–8σ) than the Mo–O3 bond length. The effect is greater for the $p\text{-CH}_3$ and $p\text{-Cl}$ complexes than for the parent $p\text{-H}$ compound. The Mo–O1–C angles for the extended phenolato ligands are similar to one another ($130.5(3)^\circ$, $\text{X} = \text{Me}$; $134.7(3)^\circ$, $\text{X} = \text{H}$; $131.5(3)^\circ$, $\text{X} = \text{Cl}$) and to the Mo–O–C angle of the single extended phenolate group of $\text{LMoOCl}(\text{OC}_6\text{H}_4\text{CN})$ ($133.9(6)^\circ$).²² However, the Mo–O3–C angles for the phenolato groups that lie between two pyrazole rings are substantially greater for the 4-methyl- and 4-chloro-substituted phenolato complexes ($145.9(3)^\circ$, $\text{X} = \text{Me}$; $145.3(3)^\circ$, $\text{X} = \text{Cl}$) than for $\text{LMoO}(\text{OC}_6\text{H}_5)_2$ ($136.6(3)^\circ$). The association of the larger Mo–O–C angle with the larger Mo–O distance is unexpected. In many reported

structures of compounds containing phenolato ligands^{23–30} the shorter M–O distances are associated with larger M–O–C angles, and the correlation has been ascribed to the ability of an aryloxo ligand to participate in a resonance form of the type $\text{M}=\text{O}=\text{Ar}$.³¹ On the other hand, several niobium(V) and tantalum(V) complexes have been reported that show no correlation between the M–O–C angle and the M–O distance.^{32–37} Consequently, the M–O–C bond angle does not necessarily correlate with the amount of π donation to the metal atom^{32,38} and may be influenced by small changes in the steric environment.

Electronic Absorption Spectra. The electronic absorption spectral data for **1–10** in 1,2-dichloroethane solution are listed in Table II. The compounds exhibit a wide range of colors: dark ruby-red for $\text{X} = \text{Me}$, Et , and H ; dark brown for $\text{X} = \text{OMe}$, OEt , and OH ; reddish for $\text{X} = \text{F}$, Cl , Br , and I ; and bright orange for $\text{X} = \text{CN}$. The electronic absorption spectra in the range 900–400 nm display two absorption bands. The lower energy band is relatively weak in intensity ($\epsilon \leq 130 \text{ L mol}^{-1} \text{ cm}^{-1}$) and always partially overlapped by the second absorption band at higher energy which is quite broad and intense ($\epsilon > 1750 \text{ L mol}^{-1} \text{ cm}^{-1}$). The former one is ascribed to a ligand-field transition and the later to a ligand-to-molybdenum (probably phenoxide-to-molybdenum) charge-transfer band. Compared to the optical spectrum (Figure 3) of the unsubstituted phenolato compound, $\text{LMoO}(\text{OC}_6\text{H}_5)_2$,¹³ the para-substituted phenolato compounds containing electron-donating substituents exhibit bathochromic shifts in the ligand-field and charge-transfer transitions, whereas the electron-withdrawing substituents induce hypsochromic shifts.

A plot of the energy of the lowest energy charge-transfer band ($\tilde{\nu}$) versus the substituent constant (σ_p)³⁹ gives a correlation coefficient of 0.980 (Figure 4a and eq 2). A plot of the energy

$$\tilde{\nu} (\text{cm}^{-1}) = 2652(\sigma_p) + 19746 \quad (2)$$

of the ligand-field band (Figure 4b) versus the substituent constant (σ_p) follows the same trend as the lowest energy charge-transfer band but is much less sensitive to the nature of the para substituent. The variation of $\tilde{\nu}$ with σ_p is consistent with the electronic nature of the para substituents on the phenolato ligands. Electron-withdrawing substituents (F, Cl, Br, I, CN) reduce the charge density on the donor atoms, thereby stabilizing the ligand-based orbitals and shifting the oxygen-to-molybdenum charge-transfer transitions to higher energy. In contrast, electron-donating

- (18) Mayer, J. M. *Inorg. Chem.* **1988**, *27*, 3899–3903.
 (19) Kipke, C. A.; Cleland, W. E., Jr.; Roberts, S. A.; Enemark, J. H. *Acta Crystallogr.* **1989**, *C45*, 870.
 (20) Chang, C. S. J.; Pecci, T. J.; Carducci, M. D.; Enemark, J. H. *Acta Crystallogr.* **1992**, *C48*, 1096–1097.
 (21) Roberts, S. A.; Orgeta, R. B.; Zolg, L. M.; Cleland, W. E., Jr.; Enemark, J. H. *Acta Crystallogr.* **1987**, *C43*, 51–53.
 (22) Chang, C. S. J.; Carducci, M. D.; Enemark, J. H. Unpublished results.

- (23) Roberts, S. A.; Darsey, G. P.; Cleland, W. E., Jr.; Enemark, J. H. *Inorg. Chim. Acta* **1988**, *154*, 95–97.
 (24) Coffindaffer, T. W.; Rothwell, I. P.; Huffman, J. C. *Inorg. Chem.* **1983**, *22*, 2906–2910.
 (25) McCleverty, J. A.; Rae, A. E.; Wolochowicz, I.; Bailey, N. A.; Smith, J. M. A. *J. Chem. Soc., Dalton Trans.* **1982**, 951–965.
 (26) McCleverty, J. A.; Seddon, D.; Bailey, N. A.; Walker, N. W. *J. Chem. Soc., Dalton Trans.* **1976**, 898–908.
 (27) McKee, V.; Wilkins, C. J. *J. Chem. Soc., Dalton Trans.* **1987**, 523–527.
 (28) Chisholm, M. H.; Heppert, J. A.; Huffman, J. C. *Polyhedron* **1984**, *3*, 475–478.
 (29) Lubben, T. V.; Wolczanski, P. T.; Van Duyne, G. D. *Organometallics* **1984**, *3*, 977–983.
 (30) Churchill, M. R.; Fettingner, J. C.; Rees, W. M.; Atwood, J. D. *J. Organomet. Chem.* **1986**, *308*, 361–372.
 (31) Chisholm, M. H.; Rothwell, I. P. In *Comprehensive Coordination Chemistry*; Wilkinson, G., Gillard, R. D., McCleverty, J. A., Eds.; Pergamon Press: Oxford, England, 1987; Chapter 15.3.
 (32) Coffindaffer, T. W.; Steffey, B. D.; Rothwell, I. P.; Folting, K.; Huffman, J. C.; Streib, W. E. *J. Am. Chem. Soc.* **1989**, *111*, 4742.
 (33) Steffey, B. D.; Fanwick, P. E.; Rothwell, I. P. *Polyhedron* **1990**, *9*, 963–968.
 (34) Steffey, B. D.; Chamberlain, L. R.; Chesnut, R. W.; Chebi, D. E.; Fanwick, P. E.; Rothwell, I. P. *Organometallics* **1989**, *8*, 1419.
 (35) Chesnut, R. W.; Steffey, B. D.; Rothwell, I. P.; Huffman, J. C. *Polyhedron* **1988**, *7*, 753.
 (36) Chesnut, R. W.; Yu, J. S.; Fanwick, P. E.; Rothwell, I. P.; Huffman, J. C. *Polyhedron* **1990**, *9*, 1051–1058.
 (37) Chamberlain, L. R.; Rothwell, I. P.; Folting, K.; Huffman, J. C. *J. Chem. Soc., Dalton Trans.* **1987**, 155.
 (38) Kerschner, J. L.; Fanwick, P. E.; Rothwell, I. P.; Huffman, J. C. *Inorg. Chem.* **1989**, *28*, 780–786.
 (39) Jaffé, H. H. *Chem. Rev.* **1953**, *53*, 191–261.

Table II. Electronic Spectra Data^{a,b}

compound	$\tilde{\nu}$ ($\times 10^3$ cm ⁻¹)	λ (nm)	ϵ (L mol ⁻¹ cm ⁻¹)
1	13.04	767	119
	19.38	516	1790
	28.57 (sh)	350	8020
	32.05 (sh)	312	9450
	34.84 (sh)	287	9740
2	40.00 (sh)	250	16490
	12.99	770	130
	19.12	523	1790
	28.90 (sh)	346	7690
	33.11 (sh)	302	8760
3	35.21 (sh)	284	10060
	41.15 (sh)	243	20380
	12.89	776	114
	18.98	527	2080
	28.90 (sh)	346	8590
4	33.33	330	12130
	12.77	783	120
	19.01	526	1940
	28.90 (sh)	346	7040
	33.56 (sh)	298	10550
5	12.67	789	120
	18.80	532	1920
	25.51 (sh)	392	4840
	29.07 (sh)	344	6270
	33.90 (sh)	295	10350
6	13.07	762	114
	20.04	499	1760
	28.57 (sh)	350	7950
	31.55 (sh)	317	8860
	34.97 (sh)	286	12100
7	13.19	758	130
	20.45	489	2110
	28.57 (sh)	350	8640
	32.68 (sh)	306	10930
	34.97	288	12400
8	39.84	251	20920
	13.28	753	100
	20.68	484	2240
	28.57 (sh)	350	9870
	32.68 (sh)	306	12190
9	35.09 (sh)	285	13720
	13.25	756	120
	20.41	490	2270
	28.41 (sh)	352	10240
	32.57 (sh)	307	12310
10	34.46 (sh)	291	13490
	13.41	746	110
	21.19	472	2030
	28.65 (sh)	349	12500
	33.22 (sh)	301	18230
LMoO(O-C ₆ H ₅) ₂	13.30	750	90
	19.76 (sh)	506	2340
	25.71 (sh)	389	2750
	29.33 (sh)	341	10500
	33.56	298	13000

^a In 1,2-dichloroethane. ^b (sh) = shoulder.

substituents (Me, Et, OMe, OEt, OH) increase the negative charge on the donor atoms and destabilize the ligand-based orbitals; accordingly, the energies of the ligand-to-molybdenum charge-transfer bands are decreased. Concomitantly, electron-donating substituents strengthen the ligand-to-molybdenum $p_{\pi}-d_{\pi}$ interaction, destabilizing the HOMO (mainly molybdenum $4d_{xy}$ orbital in character), reducing the energy separation between the HOMO and other $4d$ -based orbitals, and causing the ligand-field transition to exhibit slight bathochromic shifts.

Possible correlations between the shifts in the electronic spectra and several different types of substituent effects (σ_p , σ_I , σ^* , σ_R)⁴⁰ were investigated in an effort to assess the importance of the inductive factor in the transmission of the substituent group effects. Complexes 1–10 show satisfactory correlation with σ_p , but not

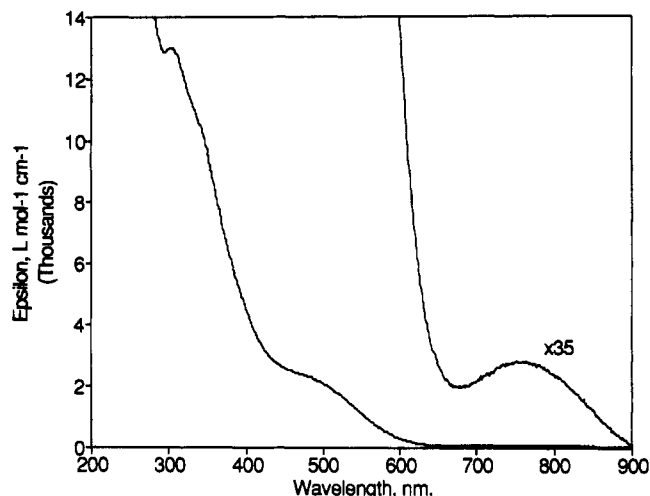


Figure 3. Electronic absorption spectrum of LMoO(OC₆H₅)₂ in 1,2-dichloroethane.

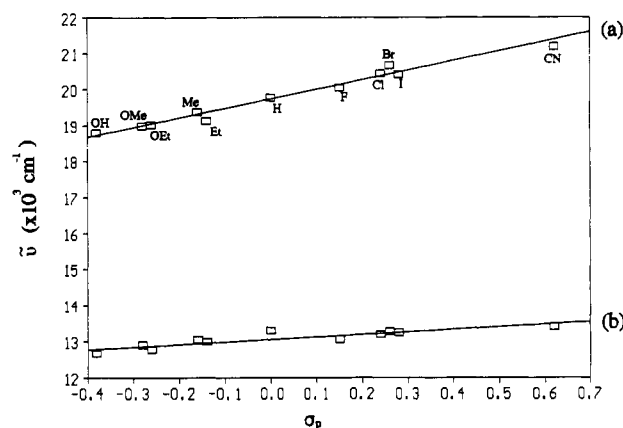


Figure 4. Correlation plot of the electronic transition energies ($\tilde{\nu}$) with the substituent constant (σ_p) for bis(para-substituted) LMoO(OC₆H₄X)₂ compounds: (a) lowest energy ligand-to-molybdenum charge-transfer band; (b) ligand-field transition.

with other parameters, indicating that the inductive factor alone cannot be solely responsible for the perturbation of the molecular properties. However, the successful correlation of the energy of the ligand-field and the lowest-energy ligand-to-molybdenum charge-transfer transitions with σ_p clearly suggests that the substituent effect is transmitted to the molybdenum atom through the phenyl ring and finally through the oxygen-to-molybdenum π -interaction.

Electron Paramagnetic Resonance Spectra. Solution EPR spectra of 1–10 at room temperature exhibit a strong central line and six surrounding hyperfine lines characteristic of Mo(V). The frozen glass-state EPR spectra at 77K for 1–10 exhibit rhombic behavior. No ligand superhyperfine splitting can be identified, suggesting that the unpaired electron is located in the nodal-plane of the equatorial N₂O₂ donor set as found for other LMoO(X,Y) complexes.

The isotropic spin Hamiltonian parameters, $\langle g \rangle$ and $^{95,97}\text{Mo}(A)$, and anisotropic g_i values for the bis(phenolato) complexes 1–10 (Table S7, supplementary material) are quite similar to one another in spite of significant shifts in both the ligand field and charge-transfer bands in the optical spectra. This relative independence of the EPR parameters to para substituents on the phenolato ligands is consistent with previous analyses of the g_i values in LMoO(X,Y) complexes.^{9,13,41} That is, the HOMO is energetically isolated from the [LMoO]²⁺ core and predominantly metal d_{xy} in character; the orbital composition of the HOMO is

(40) Exner, O. In *Correlation Analysis in Chemistry*; Chapman, N. D., Shorter, J., Eds.; Plenum Press: New York, 1978; Chapter 10.

(41) Mabbs, F. E.; Collison, D. *Electron Paramagnetic Resonance of d Transition Metal Compounds*; Elsevier: Amsterdam, 1992.

primarily determined by the nature of the two donor atoms coordinated to the $[\text{LMoO}]^{2+}$ core and is little perturbed by groups beyond the first coordination sphere. This interpretation has been suggested previously on the basis of our studies of a series of diolato and bis(alkoxo) compounds using gas-phase He I valence photoelectron spectroscopy,¹⁰ EPR,⁹ and electrochemistry.⁹

Conclusions

This work further supports the view that the $[\text{LMoO}]^{2+}$ fragment is a transferrable structural entity that imposes *fac* six-coordinate stereochemistry on the oxo-Mo(V) center. Remote substituents on an aromatic ring of $\text{LMoO}(\text{OC}_6\text{H}_4\text{X})_2$ complexes do affect the electronic spectra of the molybdenum center, but the EPR spectra show that the nature of the HOMO containing the unpaired electron is similar for all members of the series.

Structurally characterized $\text{LMoO}(\text{E}-\text{C}_6\text{H}_4-\text{X})_2$ (E = O, S) complexes show remarkably similar overall stereochemistry.

Acknowledgment. We gratefully acknowledge financial support of this research by the National Institute of Health (Grant No. GM37773). T.I.P. thanks the National Science Foundation for a summer fellowship through the REU program. We thank Dr. Katsumoto Yamanouchi and Dr. Michael A. Bruck for helpful discussions. The X-ray structure determination was performed in the Molecular Structure Laboratory of the University of Arizona.

Supplementary Material Available: Tables giving details of the structure determination of **1** (Table S1), atom coordinates (Table S2), complete bond distances (Table S3), bond angles (Table S4), anisotropic thermal parameters (Table S5), torsional angles (Table S6), and EPR parameters for **1-10** (Table S7) (11 pages). Ordering information is given on any current masthead page.